ORIGINAL ARTICLE

Mathematical modeling of electrical activity of uterine muscle cells

Sandy Rihana · Jeremy Terrien · Guy Germain ·
Catherine Marque

Abstract The uterine electrical activity is an efficient parameter to study the uterine contractility. In order to understand the ionic mechanisms responsible for its generation, we aimed at building a mathematical model of the uterine cell electrical activity based upon the physiological mechanisms. First, based on the voltage clamp experiments found in the literature, we focus on the principal ionic channels and their cognate currents involved in the generation of this electrical activity. Second, we provide the methodology of formulations of uterine ionic currents derived from a wide range of electrophysiological data. The model is validated step by step by comparing simulated voltage-clamp results with the experimental ones. The model reproduces successfully the generation of single spikes or trains of action potentials that fit with the experimental data. It allows analyzing ionic channels implications. Likewise, the calcium-dependent conductance influences significantly the cellular oscillatory behavior.

Keywords Myometrial ionic currents ·
Uterine excitability · Voltage clamp · Action potential ·
Electrophysiological model

S. Rihana (⊠) · C. Marque
CNRS, UMR 6600 Biomécanique et Bio-ingénierie,
60200 Compiègne, France
e-mail: Sandy.Rihana@utc.fr;
Sandy.Rihana@mi.parisdescartes.fr

C. Marque
e-mail: catherine.marque@utc.fr

J. Terrien
School of Science and Engineering, Reykjavik University,
Reykjavik, Iceland
e-mail: jeremy@ru.is

G. Germain
INRA, UMR 1198 Biologie du développement et reproduction,
78350 Jouy en Josas, France
e-mail: guy.germain@jouy.inra.fr

G. Germain
ENVA, UMR 1198 Biologie du développement et reproduction,
78350 Jouy en Josas, France

G. Germain
CNRS, FRE 2857, 78350 Jouy en Josas, France

1 Introduction

The uterus is usually relatively quiescent during pregnancy and conversely it exhibits rhythmic forceful contractions at term. These contractions appear because of propagated electrical activity generated at cellular levels. Different studies have demonstrated that this electrical activity is highly correlated to uterine contractions and has an important clinical potential [4, 9, 18, 19]. This electrical activity is initiated at the cellular level. Its shape and characteristics vary during pregnancy from a single spike, an irregular train of action potentials, to a regular train of action potentials observed at the end of term. Understanding the uterine electrical activity is not limited to cellular level. Indeed, uterine gap junctions play an important role in the propagation. In fact, during pregnancy, the propagation is limited due to the lack of gap junctions and at the end of term, before delivery, an abrupt increase in gap junctions is significantly observed [10]. Our aim was to develop a physiological model of the uterine electrical activity in order to correlate these physiological mechanisms, in terms of genesis and propagation of the uterine electrical activity to the recorded uterine electromyogram EMG. This paper will focus on describing the model developed first at the cellular level.

The cellular electrical activity, difference of potential across the cell membrane, is due primarily to the unequal distribution of ions between the intra- and extra-cellular spaces.

The understanding of impulse generation in uterine cell, like in many types of excitable cells, lies on the concept of changes in ionic permeability of the excitable membrane [11]. The core framework of modeling excitable cell functioning was raised 50 years ago as the Hodgkin–Huxley model of the giant axon [11]. Over the past decades, the history of modeling was widely developed in nerve and heart tissue. In 1962, Noble [23] proposed the first model of cardiac tissue (Purkinje fibers) based on Huxley and Hodgkin formulations. Cardiac tissue models were continuously improved with the progress of the different experimental techniques and the study of the biophysical properties of its cell membranes.

However, so far, few models concerning the myometrial ionic channels and their activity control had been developed. Previous models of the myometrium have been developed at the organ level [1, 34] based on automaton discrete cell states. Ramon et al.[10] presented an electrophysiological model of smooth muscle based on Huxley and Hodgkin [6]. This model was limited to sodium and potassium voltage-dependent currents and was not based on the physiological ionic currents involved in the myometrial excitation. Recently, Bursztyn et al. [5] published an excitation-contraction model of uterine muscle cells. This mathematical model reports the cellular mechanisms of calcium control such as L-type voltage-dependent current, Ca^{2+} pumps and Na^+/Ca^{2+} exchangers. However, it neglects the inactivation process of calcium current, the time dependency of kinetic dynamics and all other ionic mechanisms involvedsuch as potassium and sodium. In this paper we present a model of the uterine excitability involving the main ionic mechanisms responsible for the genesis of the uterine excitability. The data in the model are based on the electrophysiological properties of the uterine cell. Therefore, the adaptation of voltage clamp experiments is a major forward step. The most important advantage of voltage-clamp is that it eliminates the capacitive current and reduces all membrane currents to the ionic ones. This technique allows, by blocking membrane ionic channels, leaving a single channel active to identify the principal kinetics that govern its corresponding ionic current.

The major key for physiological modeling is a better understanding of the main physiological processes involved. Therefore, our methodology is described as follows: first, we present a basic review of the main biophysical properties of the uterine cell and of its main ionic channels. Then, we develop the modeling steps and show how we have compiled all the ionic channels data obtained from the uterine voltage clamp experiments to formulate equations for the main myometrial ionic currents, based on the fundamental electrophysiological principles developed on the giant squid axon by Huxley and Hodgkin (HH) in 1952 [11]. These equations serve to develop a physiological model of the uterine electrical activity of a single cell that is presented in this paper.

2 Methods

During pregnancy, uterine cells are generally quiescent and characterized by a resting membrane potential V_m varying slightly under hormonal influences. It passes throughout pregnancy from −60 mV at mid term, to −45 mV at term [8, 27]. In some uterine cells, a spontaneous depolarization occurs, the pacemaker potential, in addition to the resting membrane potential. When the depolarization exceeds a threshold, the cell shows a single spike, a plateau, regular train of spikes or irregular one. The alternation between resting state and repetitive single spikes is known as bursting behavior. This is especially observed at the end of gestation [27].

The frequency of the burst discharges and the number of spikes in each burst vary considerably, and are largely influenced by hormonal and gestational factors as well as by pharmacological agents. Burst discharge frequency and spike frequency within bursts have values in rat at term (1.2 bursts/min and 1.5 spikes/s, respectively) [10, 20] that are different to earlier stages of pregnancy (0.45 burst/min and 4 spikes/s, respectively). The duration of bursts is shorter at delivery (21.5 s), when compared to earlier stages of pregnancy (32 s) [10, 20]. On a single cell level, myometrial single action potential (AP) recorded after a short depolarizing pulse has a duration of approximately 133 ms [13]. In response to longer depolarizing pulse, a burst of action potential is observed and the AP duration is increased to approx. 200–250 ms. The increase in the action potential amplitude due to the longer depolarizing pulse can be explained by the different time constants of each individual myometrial cells and the charges concentrated in the capacitance membrane of the myometrial cell. The spiking activities present peak amplitude of 54.6 mV in depolarized cells [13]. The electrical activity is modulated by the activity of the myometrial ion channels and by the dynamics of the intracellular concentration. A brief description of these processes will be given.

2.1 Myometrial ion channels

The main myometrial ionic channels, responsible for the excitability of the cells, and their activity are briefly described below.

2.1.1 Sodium voltage dependent channels

These channels have been described in rat and human myometrial cells [33, 35]. Sperelakis et al. [30] postulated that these channels contribute with gap junctions, to the pacemaker potential generation and to a complete rhythmic forceful propagation of the electrical activity at the time of parturition.

2.1.2 Calcium voltage dependent channels

At least two types of calcium voltage-dependent currents have been described in the smooth muscle [31].

- L type channels (Long lasting): They are predominant in the rat uterine myocytes [21, 33]. L-type Ca^{2+} channels are associated with Ca^{2+} entry in the intra-cellular space and consequently with the contraction in the myometrium.
- T type channels (Transient): These channels are associated with transient currents. They are described in human uterine cells [12, 36]. They are activated only by depolarizing pulses from a holding potential of -100 mV and completely inactivated at toward -60 mV. Thus, for a resting potential of -50 mV, a large fraction of the transient type calcium channel is inactivated, raising the question of its physiologic role in the generation of action potential [12, 36].

Otherwise, they are rarely observed in rat myometrial pregnant cell. The presence of these channels is generally linked to action potential generation and pacemaker activity [12, 36].

2.1.3 Potassium channels

The role of potassium channels in the control of the uterine excitability is not still completely understood [23, 25]. Nevertheless, it is obvious that these channels contribute primarily to the repolarization of the cell after an action potential [15, 28, 32]. The importance of K^+ channels, in maintaining the resting membrane potential, and in the repolarization, is related to the long period of some hundreds of milliseconds of channel activation [32]. Two primary types of potassium channels have been described in the myometrium: potassium voltage-dependent channels and potassium calcium dependent channels [14, 32].

2.1.4 Chloride channels

These channels have not been extensively evaluated although they play an important role by controlling the repolarization of the uterine activity [28]. The plateau observed in some depolarization of uterine cells is almost equal to the chloride equilibrium potential [7]. The chloride current still activated like a background current. Apart from its contribution in the repolarization of the cell, it may play an important role in the depolarization of the membrane [3]. This depolarization may contribute in its turn to the opening of voltage-dependent calcium channels.

2.2 Intracellular calcium concentration

Intracellular calcium plays an important role in the modulation of myometrial electrical activity. Ca^{2+} may be seen as the main transporter of charges in a uterine cell. Ca^{2+} plays a major role in the modulation of the electrical uterine activity throughout pregnancy. Like in other smooth muscles, the contractility of uterine muscle cells is largely dependent on the intracellular free calcium concentration. The rise in $[Ca^{2+}]_i$ occurs when efficient stimulation is applied and when the major entry of Ca^{2+} ions into the uterine cell is done through the L-type Ca^{2+} channels [29]. The efflux or the decrease of the intracellular calcium concentration needed for membrane repolarization, is controlled by different mechanisms such as calcium pumps, Na^+/Ca^{2+} exchangers and the calcium sequestration by the intracellular compartments. Consequently, intracellular calcium dynamics is an important component to be taken into account for the electrophysiological modeling of uterine cell activation.

## 2.3 Basic steps toward modeling

Based on the Huxley and Hodgkin model [11], the transmembrane current, I_m, can be divided into two components as shown in Fig. 1: the capacitive current, due to the bilipidic layer of the cell membrane, and the ionic current due to the flux of ions between the intra and the extra cellular space. Experimentally, I_m is equal to the stimulation current I_{stim} applied to the uterine cell. Thus, the electrical properties of the uterine cell can be described by the following differential equation 1.

$$I_{stim} = C_m \frac{dV_m}{dt} + \sum I_{ion} \tag{1}$$

where I_{stim} is the membrane stimulation current (μA/cm^2), C_m is the membrane capacitance (μF/cm^2), I_{ion} is the sum of the involved ionic currents (μA/cm^2), and V_m is the transmembrane potential, the difference between the intracellular potential and the extracellular potential (mV).

For the myometrial cell, taking into consideration the main ionic channels described above, the total ionic current, I_{ion} can be expressed as follows (Eq. 2):

$$I_{ion} = I_{Na} + I_{Ca} + I_{K(V)} + I_{K(Ca)} + I_L \tag{2}$$
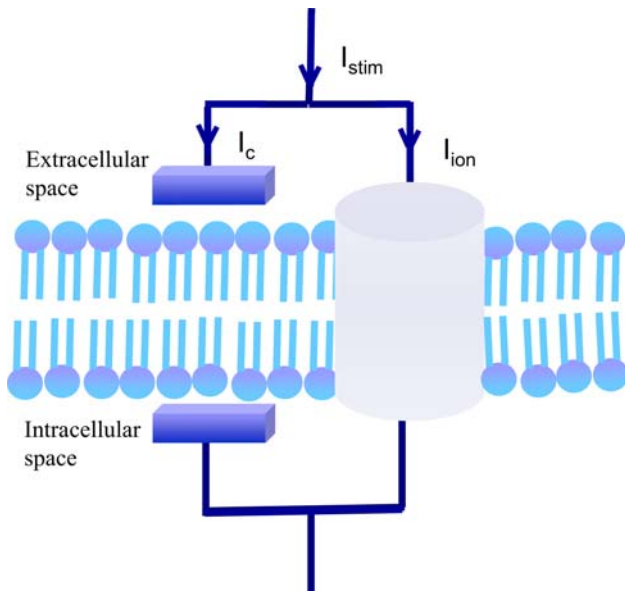
Fig. 1 Current membrane circuit. Uterine cell transmembrane current divided in capacitive and ionic currents, based on the Huxley and Hodgkin [6] core framework of the electrophysiological modeling

I_{ion} is divided into inward and outward currents. Inward current is composed primarily of sodium and calcium voltage-dependent currents, I_{Na} and I_{Ca} respectively. Potassium voltage-dependent current $I_{K(V)}$, potassium calcium-dependent current $I_{K(Ca)}$ and leakage current I_L mainly constituted of chloride ions, form the outward current.

Each ionic current, I_i (i = Na, Ca, K(V) or K(Ca)), is assumed to be related to the membrane voltage, V_m, based on the voltage-dependent gating properties (Eq. 3).

$$I_i = g_i(V_m - E_i) \tag{3}$$

where g_i is the ionic conductance (mS/cm^2), E_i is the equilibrium potential of the ion i (mV) and is defined by the Nernst equation.

Figure 2a shows the electrical circuit diagram representative of the uterine cell membrane and how the total membrane ionic current I_{ion} is subdivided into individual ionic currents I_i. The conductances, g_i, are defined by the Huxley and Hodgkin formulations for each ionic channel and the voltage generators. All ionic conductances, g_i (unless g_L), are considered as time dependent. The time dependence is indicated by the activity of the activation and inactivation gates that modulate the state of the channel. In the HH model, these gates are governed by variables; each variable presents the probability of which a gate is permeant to ions. It varies between 0 (fully non-permeant to ions) and 1 (fully permeant to ions). As an illustration, a channel, i, is fully open when all gates are open. Therefore, g_i is assumed to be proportional to the product of the probability of open

channels, $m^x h^y$, the probability of the all-gating variables (x activating gates with an m probability, and y inactivating ones with h probability), and proportional also to the maximal ionic channel conductance, G_i, thus giving rise to the following Eq. 4.

$$I_i = G_i m^x h^y (V_m - E_i) \tag{4}$$

The variation of each gating variable (m or h) can be expressed by first order differential equation 5.

$$dm/dt = (m_\infty - m)/\tau_m$$
$$dh/dt = (h_\infty - h)/\tau_h \tag{5}$$

where τ_m and τ_h are relaxation times, m_∞ and h_∞ denote the activation and inactivation steady states. Both steady states follow a distribution described by Eq. 7 (Boltzman distribution).

$$m_\infty = 1/(1 + \exp((V_m + V_{1/2})/S))$$
$$h_\infty = 1/(1 + \exp((V_m + V_{1/2})/S)) \tag{6}$$

$V_{1/2}$ is the half activation potential and S is the slope factor.

Figure 2b presents a schematic description of the model of the uterine cell, including the ionic channels involved, and the activation and inactivation kinetics of a single ionic channel.

Holding the membrane potential at a certain value (V_c), eliminates the capacitive current and thus the ionic currents can be studied separately. Our study is based on the evolution of the ionic currents in response to an instantaneous depolarization of the transmembrane potential, different quantitative characteristics such as ionic current equations, and time constants. Steady-state parameters can be extracted and used to carry out an electrophysiological realistic model. The steps toward modeling can be described briefly as follows, e.g., for the sodium voltage-dependent current.

2.3.1 Time evolution of ionic current expressions

For each ionic channel, our work is based on the current–time relationships, the temporal activation, or inactivation ionic current expression found in the literature such as the following equation (Eq. 7), describing the temporal activation of sodium current [33], and assuming the existence of four activating gates for Na channels.

$$I = I_\infty (1 - \exp(-t/\tau))^4 \tag{7}$$

From the time–current relationship, the evolution of time constants values in function of the holding membrane potential give the expression of the time constant expressions such as the time constant τ, in Eq. 8, describing sodium time activation in function of transmembrane potential V_m. We estimated the mathematical equation expression that could

Fig. 2 Single uterine cell model. **a** Electrical circuit diagram of the uterine membrane cell based on the literature and on the Huxley and Hodgkin basics [11]. **b** *Left panel* a general schematic picture of the ionic channels involved in uterine excitability, with emphasis on the intracellular calcium concentration dynamics due to the influx of Ca^{2+} through the Ca^{2+}-voltage-dependent channels and the sequestration of these ions by the intracellular compartments. *Right panel* kinetics (activation and inactivation gates) of each ionic channel
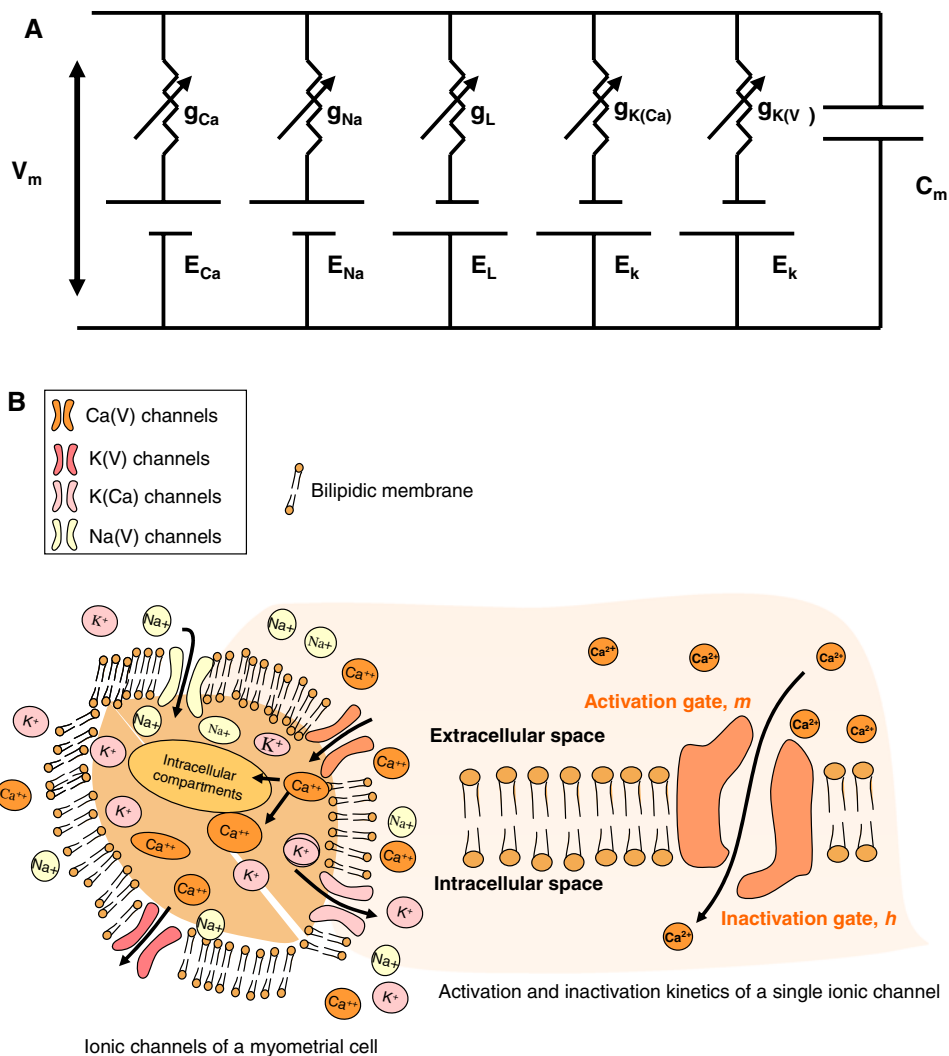

fit with the experimental data described by Yoshino et al. [33] The following equation expresses the sodium activation time constant shown in Fig. 3 and its expression, described by

$$\tau_{mNa} = 0.25 e^{(-0.02 V_m)} \qquad (8)$$

Fitting procedure in MATLAB$^\circledR$ software (Matlab 7.0, Mathworks) SSE (Sum Square error) = 0.000192 R^2 (Coherence = 0.9936).

The same kind of expressions applies for other activating and inactivating gates of other ions such as sodium-inactivating gate, calcium-activating gates, and potassium-inactivating gates.

We found one sodium-inactivating gate and the expression of the time constant expressed as $\tau_{hNa} = 0.22 e^{(-0.06 V_m)} + 0.366$ *(fitting procedure in MATLAB$^\circledR$ software (Matlab 7.0, Mathworks) SSE (Sum Square error) = 0.000022 R^2 (Coherence = 0.9946).* Finally, the
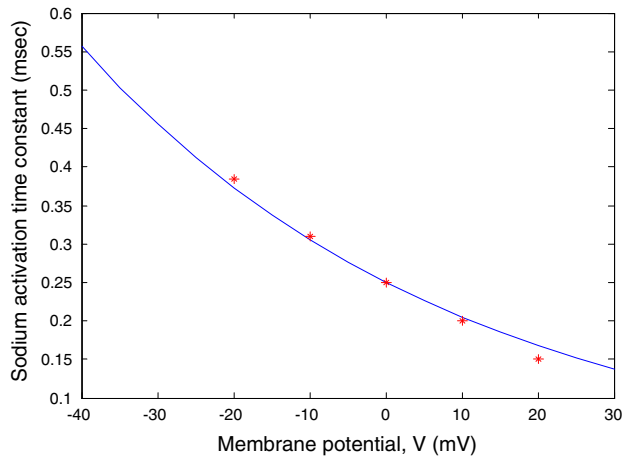
Fig. 3 Sodium activation time constant. Sodium activation time constant expression as function of the transmembrane potential. Curve fitting to the data (*stars*) extracted from Yoshino et al. [33]

sodium voltage-dependent current expression is expressed by the following equation:

$$I_{Na} = G_{Na} m_{Na}^2 h_{Na}(V_m - E_{Na}) \tag{9}$$

2.3.2 Current–transmembrane potential relationships

The current–potential relationship serves the physiologists to determine the kinetics of the activation and inactivation channels. From the experimental voltage clamp data found in Yoshino et al. [33], we found the activation and inactivation steady states of the sodium channels as described by Eq. 10.

$$m_{Na\infty} = 1 \left/ \left(1 + \exp\left(\frac{V_m + 21}{-5}\right)\right)\right. \tag{10}$$

Moreover, the sodium steady-state voltage inactivation relation follows a Boltzman distribution described as follows:

$$h_{Na\infty} = \frac{1}{(1 + \exp\left((V_m + 58.9)/8.7\right))} \tag{11}$$

2.3.3 Validation

In order to validate all the mathematical equations and the assumptions made for each ionic current, we simulated voltage-clamp experiments for ionic current using these equations. By holding membrane potential at a constant value, we compared the simulated curves (current–time and current–transmembrane potential) with the experimental ones found in the literature.

The same methodology was used for the other ionic currents:

2.3.4 Calcium voltage-dependent current

Calcium currents in pregnant rat uterine myocytes are mainly of L-type [21, 24, 33]. They are responsible for the influx of calcium ions to the intracellular space and consequently for the intracellular calcium concentration increase. The activation of I_{Ca} has been described in [33] by a square function (number of activations gates equal to two). We fitted the voltage-dependent time constant τ with an exponential equation $\tau_{mCa} = 0.64 \exp(-0.04 V_m) + 1.188$.

Calcium inactivation is more complex than sodium inactivation. Young et al. [36], have found a great cell-to-cell variability for the decay time course of the L-type current. Most of cells were found expressing an inactivation time of the order of tens of milliseconds. These data of the inactivation times of woman calcium currents I_{Ca} [36], are in agreement with the results found by Yoshino et al. [33], in pregnant rat uterine cells. In this case, inactivation time τ has been described by two exponential phases. The first one, voltage-dependent, is the faster, τ_f, showing a U-shaped relationship indicative of an effect of Ca^{2+} in calcium channel inactivation. In addition, the expression of this time constant could be expressed by the sum of two exponentials described by the following equation:

$$\tau_f(V) = a \exp\left(-\left(\frac{V_m - b}{c}\right)^2\right) + d \exp\left(-\left(\frac{V_m - e}{f}\right)^2\right) + g \tag{12}$$

with $a = 35.05$, $b = 13.61$, $c = 12.34$, $d = 134.7$, $e = 103.8$, $f = 52.14$, $g = 27.74$.

The second one, τ_s, may have some voltage dependence. However, the data recovered from the literature are too scattered [33] to define its exact scalar value. Because it is also the slower one, it can be considered as a constant mean value, of about 160 ms. Because 38% of the calcium current is quickly inactivated and 22% consists the slow current inactivated, we assume the inactivation calcium gate is expressed by the following Eq. 13:

$$h_{Ca} = 0.38 h_{Caf} + 0.22 h_{Cas} + 0.06 \tag{13}$$

In addition, the steady-state voltage inactivation relation follows a Boltzman distribution described by Eq. 14.

$$h_{Ca\infty} = 1/(1 + \exp((V_m + 34)/5.4)) \tag{14}$$

2.3.5 Potassium voltage-dependent current

Three populations of K^+ voltage-dependent current have been described by Wang et al. [32] (I_{K1}, I_{K2}, I_{K3}). Two have inactivating components and the third one is noninactivating and represents the 10% left of the total I_K. $I_{K(V)}$ could be described by the sum of the three components. The activation and inactivation kinetics of these currents were fitted to the ones found in the literature [32]. Some time-scale values are too long relatively to the uterine time scale excitability such as first potassium component inactivation time constant ($\tau_{hK1} > 2.5$ s) [32], which is ten times larger than uterine action potential duration (<300 ms). We therefore simplified the equations by neglecting this inactivating gate. Other time constants are too short and nearly instantaneous relative to uterine action potential duration. It is the case of the third activation potassium n_{K3}, which is instantaneously activated. Therefore, we set its value at its steady-state value due the fact that it reaches quickly.

2.3.6 Potassium calcium-dependent current and intracellular calcium concentration

These channels, both Ca^{2+} and voltage-dependent, might contribute to membrane repolarization after membrane

depolarization and to $[Ca^{2+}]_i$ rise [2]. P_0, the ratio between the open duration time and the total time channel, fits the Hill function (Eq. 15).

$$P_0 = \frac{1}{(1 + (K_{1/2}/[Ca^{2+}]_i)^N)} \tag{15}$$

where $K_{1/2}$ is the concentration of half-activation and N is the Hill coefficient. $K_{1/2}$ is about 10 μM at −40 mV and 20 μM at −50 mV, $N = 2$, for both potentials [2].

Based on Eq. 3, we used the following I_{KCa} expression (Eq. 16).

$$I_{K(Ca)} = g_{K(Ca)}(V_m - E_k) \tag{16}$$

where $g_{K(Ca)}$, the total K(Ca) channel conductance, is expressed as the product of the maximal K(Ca) conductance $G_{K(Ca)}$ by the probability of the channel to be open and is function of $[Ca^{2+}]_i$ and can be expressed as follows (Eq. 17).

$$g_{K(Ca)} = G_{K(Ca)} \left(\frac{[Ca^{2+}]_i^N}{(K_d^N + [Ca^{2+}]_i^N)} \right) \tag{17}$$

K(Ca) channels are membrane voltage and intracellular calcium concentration dependent. A simple mathematical model of the form presented in Eq. 18 describes the dynamics of the intracellular calcium concentration. f_c in Eq. 18 is the probability of the influx of Ca^{2+} participating in the concentration dynamics, α is a factor of conversion from influx Ca^{2+} current $I_{(Ca(V))}$ to ionic concentration per time, and K_{Ca} represents the sequestration, extrusion, and buffering processes of Ca^{2+} by the intracellular compartments [6].

$$\frac{d[Ca^{2+}]_i}{dt} = f_c(\alpha I_{Ca} - K_{Ca}[Ca^{2+}]_i) \tag{18}$$

2.3.7 Uterine cell model

Based on the ionic currents described previously, we can state that the main ionic currents involved in myometrial cell activity are

1. Sodium voltage-dependent current I_{Na}.
2. Calcium voltage-dependent current responsible for most inward current during an action potential, mostly a long lasting calcium current I_{CaL}.
3. Voltage-dependent potassium current predominately responsible for membrane repolarization, $I_{K(V)}$, described by the sum of three components $I_{K1(V)}$, $I_{K2(V)}$ and $I_{K3(V)}$.
4. Calcium-activated-K^+ current, $I_{K(Ca)}$.

Besides these currents, I_L denotes leakage current including the remaining ionic current. I_{stim} represents the stimulation current, the external current applied to the membrane cell. By including the equations related to ionic currents described below, we obtained a set of first differential equations describing the activation and inactivation kinetics' temporal variations. The ten simple differential equations presented in Eq. 19, describe the temporal variation of the dynamics of the model.

$$dV/dt = (I_{stim} - I_{ion}(V, m_{Ca}, h_{1Ca}, h_{2Ca}, n_K, [Ca^{2+}]_i))/C_m$$
$$dm_{Na}/dt = (m_{Na\infty}(V) - m_{Na})/\tau_{mNa}(V)$$
$$dh_{Na}/dt = (h_{Na\infty}(V) - h_{Na})/\tau_{hNa}(V)$$
$$dm_{Ca}/dt = (m_{Ca\infty}(V) - m_{Ca})/\tau_{mCa}(V)$$
$$dh_{1Ca}/dt = (h_{Ca\infty}(V) - h_{1Ca})/\tau_{h1Ca}(V)$$
$$dh_{2Ca}/dt = (h_{Ca\infty}(V) - h_{2Ca})/\tau_{h2Ca}(V)$$
$$dn_{k1}/dt = (n_{k1\infty}(V) - n_{k1})/\tau_{nk1}(V)$$
$$dn_{k2}/dt = (n_{k2\infty}(V) - n_{k2})/\tau_{nk2}(V)$$
$$dh_{k1}/dt = (h_{k1\infty}(V) - h_{k1})/\tau_{k1}(V)$$
$$d[Ca^{2+}]_i/dt = f_c(\alpha I_{Ca}(V, m_{Ca}, h_{1Ca}, h_{2Ca}, [Ca^{2+}]_i)$$
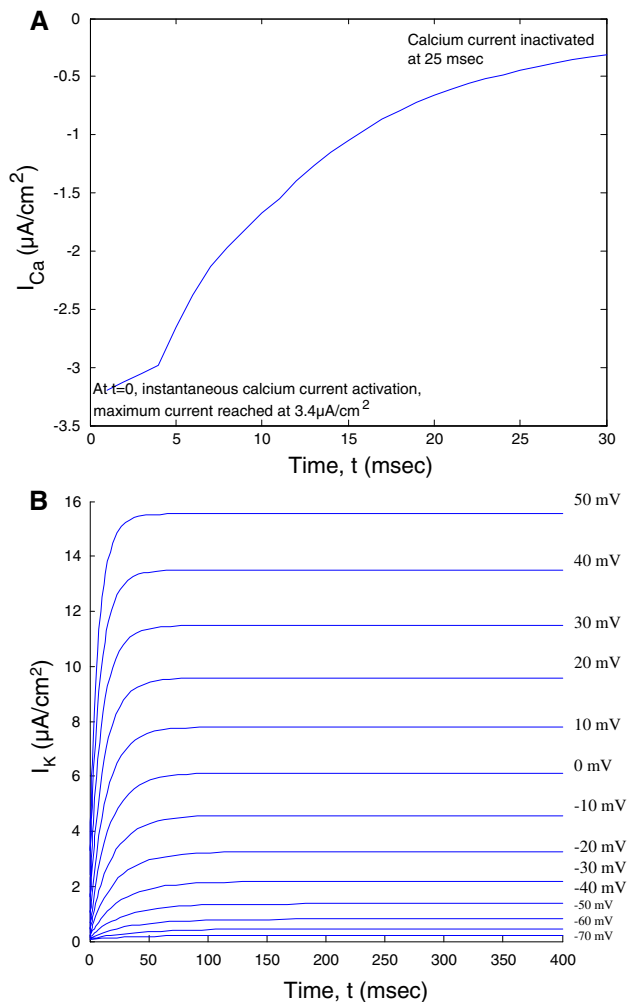$$- K_{Ca}[Ca^{2+}]_i) \tag{19}$$

where m_{Na}, h_{Na} are sodium voltage-dependent activation and inactivation kinetics, m_{Ca} calcium activation kinetic, h_{1Ca}, h_{2Ca} represent the two slow and fast calcium inactivation kinetics; n_{K1} and n_{K2} are the activation kinetics of both potassium voltage-dependent components; h_{K1} is the inactivation kinetic of the first potassium voltage-dependent component; $m_{Na\infty}$, $h_{Na\infty}$, $h_{1Ca\infty}$, $h_{2Ca\infty}$, $n_{K1\infty}$, $h_{K1\infty}$ and $n_{K2\infty}$ represent the steady states of the variables; τ_{mNa}, τ_{hNa}, τ_{mCa}, τ_{h1Ca}, τ_{h2Ca}, τ_{nK1}, τ_{hK1} and τ_{nK2} denote the time constant; f_c, α and K_{Ca} parameters govern the influx of Ca^{2+} ions to the cell as well as the sequestration, extrusion, and buffering part of the cation, related to the intracellular compartments.

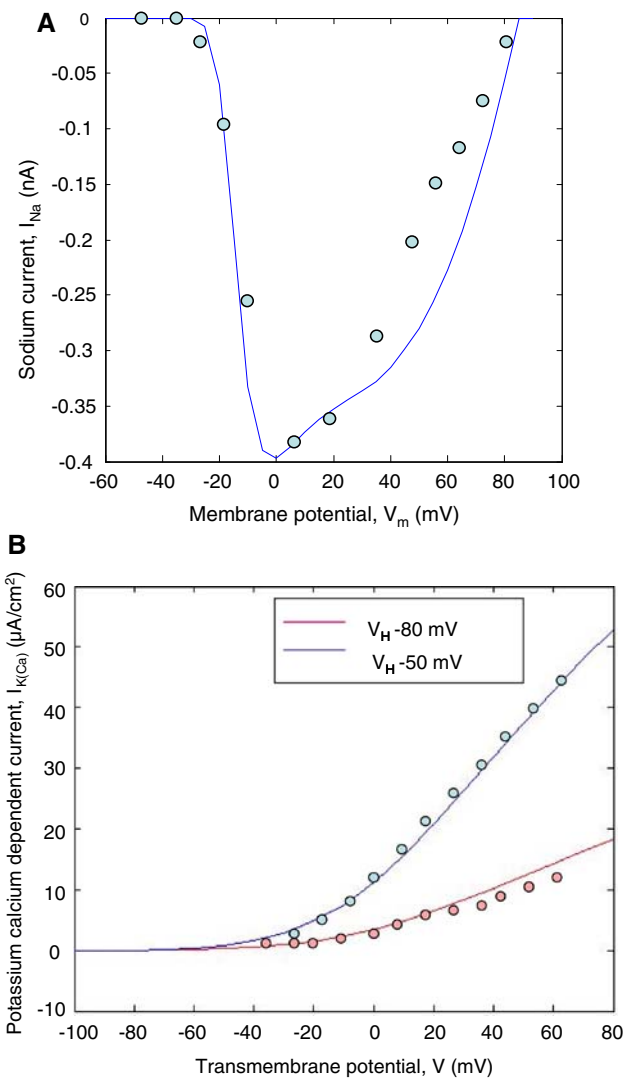### 2.3.8 Computational aspects

This type of model is a system of stiff, nonlinear ordinary differential equations that must be solved numerically. Techniques used for solving this kind of problems were those described by Moore and Ramon [22], which include fourth order Runge–Kutta method and methods with adaptive time step like the Gear method. We used the Gear method purely built-in MATLAB® routine, MATLAB's 7.0 (The Mathworks) ode15 s method. The validity of our single uterine cell model was studied step by step, by verifying the current voltage relationships of a simulated voltage-clamp experiment and comparing the relationship curve simulated for each ionic current obtained with real data (found in the literature).

For the simulated voltage clamp results, the membrane potential was held at a constant value and then depolarized by various voltage-clamp sets which represented a variation

in the transmembrane current. In order to obtain the curve fitting of each ionic current of the model for each depolarization potential, the differential equations characterizing the gating variables for each current were integrated numerically, giving thus the temporal variation of the corresponding ionic current at the denoted voltage-clamp as shown in Fig. 4a, b. Then, the parameter values were substituted into the appropriate equation for each ionic current. The graphs on Fig. 5a, b illustrate the resulting current voltage relationship obtained for Na and K ionic currents. The resulting figures fit with the experimental data found in the literature, where the critical decision parameters are the activation voltage of the current, its maximal value and the voltage corresponding to this maximum, the general shape of the curve, and the reversal potential.

Fig. 5 Ionic currents–transmembrane voltage relationships. **a** Sodium voltage-dependent current fitted to data reported by Miller et al. [20]. Criterion parameters used for the similarity: (1) Activation current at about −30 mV, (2) maximum current (0.35 µA/cm² equivalent to 0.5 nA found in Yoshino et al. [33]), (3) I_{max} reached between 0 and 10 mV, (4) reversal current, where current passes by zero at approximately 85 mV. **b** I(K)–V relationship of maximum currents obtained at two different holding potentials $V_H = -50$ mV and $V_H = -80$ mV. Fittings relative to data reported by Wang [32] (*circles*)

3 Results

The model was studied under current stimulation amplitude (at $t > 0$). The model response shows a plateau at the resting membrane potential or slightly higher, a single action potential response at higher current stimulation values or a train of peaks of action potentials.
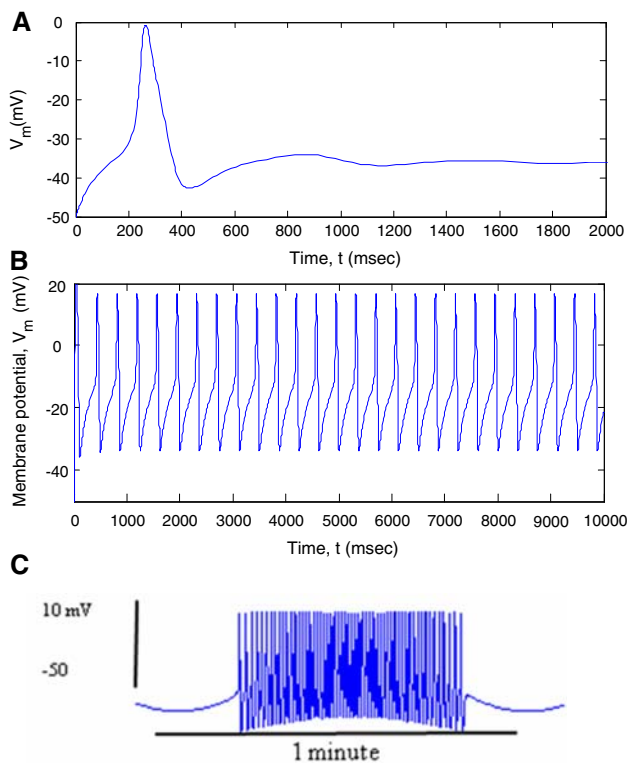
3.1 Simulated action potentials

In Fig. 6a, the model exhibits a single action potential, for I_{stim} equal to 0.1 µA/cm². When I_{stim} is above a threshold

Fig. 4 Temporal ionic current variation. **a** Temporal variation of calcium current simulated at depolarization potential 10 mV. Note the instantaneous activation of I_{Ca} and its slow inactivation. **b** K(V) currents obtained at holding potential −80 mV depolarized in 10 mV increments to −70 mV. Note the long activation time of these channels

value around of 0.12 µA/cm^2, we obtain a regular spiking. Figure 6b, shows a train of action potentials obtained for 0.2 µA/cm^2 current stimulation similar to the activity observed at term.

The difference of amplitude of the first peak with the following ones is due to the time needed for the numerical integration method to converge. It reflects the instantaneous transfer of the system, the uterine cell, from the resting membrane potential around −50 mV to the oscillatory behavior, due to the external current applied. The sustained spikes to a plateau around −35 to −40 mV are consistent with the data described in the literature [13]. Therefore, except for the first peak, the action potential peaks obtained by simulation are similar to the one observed in the literature with an absolute peak amplitude of about 40 mV and a peak duration of about 133–200 ms [15, 25, 35]. Under sinusoidal current stimulation, the model may exhibit a burst of action potential, Fig. 6C, which in terms of peak-to-peak amplitude, spike interval and burst duration, corresponds to the one observed at end of term [15, 16, 24].

Fig. 6 Different shapes of uterine electrical activity. **a** Single action potential simulated for 0.1 µA/cm^2 current stimulation amplitude. **b** Repetitive action potentials simulated in response to a current stimulation value 0.17 µA/cm^2 higher than 0.12 µA/cm^2. **c** Burst of action potential generated by a sinusoidal stimulation current
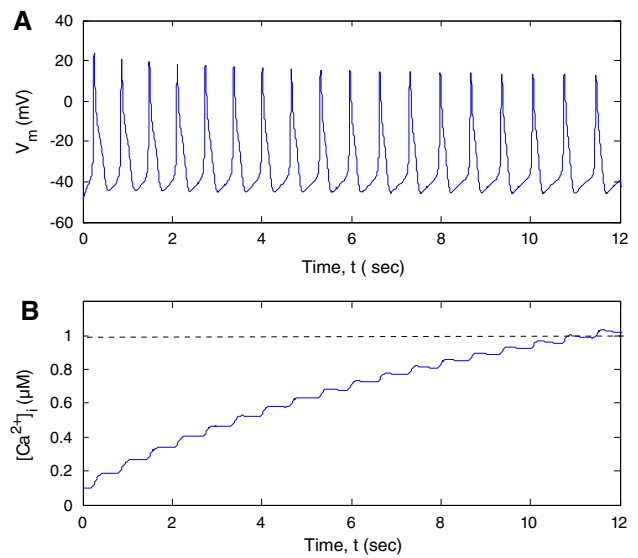
Fig. 7 Accumulation of the intracellular calcium concentration (**b**) during the sustained train of action potentials (**a**)

3.2 Intracellular calcium concentration and ionic currents

The essential core of the excitability process of a uterine cell is the intracellular calcium concentration. The influx of calcium into the myometrial cell occurs largely through the calcium voltage-dependent channel. The repetitive action potentials, as shown in Fig. 7a, are strongly associated with the opening of voltage-sensitive Ca^{2+} channels allowing the increase and the accumulation of intracellular calcium concentration. Resting intracellular calcium concentrations are between 0.1 and 0.16 µM in myometrial cells and increase in order to reach a certain threshold (between 1 and 3 mM) necessary to trigger the uterine cell contracture process [17]. This intracellular calcium concentration is illustrated in Fig. 7b.

4 Discussion

We have developed in this work an electrophysiological model representative of the electrical activity of a single uterine cell. This model is built on modified basic ionic current expressions described by Huxley and Hodgkin [11] and the data available in the literature on uterine physiology. It permitted reproducing the uterine electrical activity observed at term, and by varying the parameters such as the I_{stim} current, we produce different patterns of cell electrical activities.

Questions can be raised concerning the assumptions and simplifications that we have implemented during the development of this model.

They first concern the structure of the model itself. A perfect model would have been based on complete uterine myocyte electrophysiological data obtained from a same species and at a given stage of pregnancy. As stated above, these data are not always available. We made therefore assumptions driven from values extracted from myocytes in different species (rat, human) and from various experimental conditions. Missing parameters were finally estimated via "fine-tuning", by navigating their values in different intervals in consistence with voltage-clamp data simulating physiological conditions.

A second point of discussion is the triggering of the electrical activity. In vivo, uterine excitability is thought to be initiated spontaneously at pacemaker cells [10]. We have used in our model a stimulating current, to trigger the electrical activity of a single cell. This stimulating current was associated with the pacemaker cell. By varying the I_{stim} value, when a threshold is reached, we were able to reproduce different patterns of electrical response of the uterine cell, from a single action potential, characteristic of pregnancy, to a burst of action potentials, characteristic of the end of gestation or of labor activity. However, the duration of the burst is closely related to the duration for which I_{stim} is held, within certain limits, above the threshold. Our model allows then reproducing the single spike initiating small contractions during pregnancy and the multiple spikes that maintain large contractions at the end of gestation, but it is not yet able to reproduce the phenomenon involved in the triggering of pacemaker activity. Hence, by injecting the stimulation current, the model exhibits the electrical activity of a uterine as pacemaker cell. However, neglecting the current stimulation parameter, the cell is considered as pacefollower, and does not exhibit any electrical activity unless stimulation arises from its neighbor cells. This case will be modeled in a further work describing the propagation of electrical activity.

Conversely, by keeping constant the stimulation current, a reduction of the extra cellular calcium concentration inhibits the repetitive action potential shape and shows a single action potential, plateau-type. This confirms the important role played by the influx of calcium ions in the generation of the action potential. Therefore, a new question can be raised: could the T-type transient calcium currents be responsible for spike generation and the triggering of uterine excitability, as it is the case in cardiac and skeletal myocytes where they contribute to membrane cell depolarization and to the pacemaker activity? The importance of the T-type Ca^{2+} channels in uterine myocyte is still elusive due to the fact that a large fraction of these channels is inactivated at -60 mV [12]. It raises the question of the physiological role of these channels at a uterine resting potential of approximately -50 mV. It has been demonstrated by Schmigol et al. [29] that the major source of Ca^{2+} ions entering the cell increasing the $[Ca^{2+}]_i$ is due to the influx of L-type Ca^{2+} current. This hypothesis may justify the limitation of modeling to the L-type Ca(V) channels and neglecting the Ca^{2+}-release from the intracellular compartments.

All these questions on the model limitations still need to be clarified. To solve the problems cited above, the only way will be to go back to real voltage-clamp experiments in order to validate the assumptions made and to bring to the model the lacking data. Nevertheless, the model can be used from now in different ways. It can help understanding the contribution of myometrial ionic channels during the pregnancy and parturition. Even at this early stage of development, the model can be used to study the effect of drug injections or the effect of the association of molecules on the uterine cell behavior. We may explore, for example by using this model, the response of the cell following the administration of potassium-channel openers and of calcium inhibitors. Thus, the model can serve as an experimental platform to predict the effect of tocolytic treatments. Future collaborations with physiological and pharmacological laboratories will be held in order to validate the tocolytics treatment.

5 Conclusion

Based on myometrial voltage-clamp experiments described in the literature, we have selected the main uterine ionic currents, and proposed their voltage channel dynamic expressions to develop a mathematical model of the uterine cell excitability. Our future efforts will focus on analyzing the impacts of these parameters on the model response, in order to reduce the model and to simplify its computation. Since abdominal recording of the electrical activity of the uterus allows monitoring the uterine contractility during pregnancy [19], the final aim will be the modeling of a surface uterine electromyogram in order to correlate the characteristics of this signal to the involved physiological mechanisms.

References

1. Andersen HF, Barclay ML (1995) A computer model of uterine contractions based on discrete contractile elements. Obstet Gynecol 86(1):108–111. doi:10.1016/0029-7844(95)00111-4

2. Anwer K et al (1993) Calcium-activated K⁺channels as modulators of human myometrial contractile activity. Am J Physiol 265(4 Pt 1):C976–C985

3. Arnaudeau S, Lepretre N, Mironneau J (1994) Chloride and monovalent ion-selective cation currents activated by oxytocin in pregnant rat myometrial cells. Am J Obstet Gynecol 171(2): 491–501

4. Buhimschi C et al (1998) Uterine activity during pregnancy and labor assessed by simultaneous recordings from the myometrium and abdominal surface in the rat. Am J Obstet Gynecol 178:811–822. doi:10.1016/S0002-9378(98)70498-3

5. Bursztyn L et al (2007) Mathematical model of excitation–contraction in a uterine smooth muscle cell. Am J Physiol Cell Physiol 292(5):C1816–C1829. doi:10.1152/ajpcell.00478.2006

6. Chay TR, Keizer J (1983) Minimal model for membrane oscillations in the pancreatic beta-cell. Biophys J 42(2):181–190

7. Coleman HA, Parkington HC (1987) Single channel Cl⁻and K⁺currents from cells of uterus not treated with enzymes. Pflugers Arch 410(4–5):560–562. doi:10.1007/BF00586540

8. Coleman HA, Parkington HC (1990) Hyperpolarization-activated channels in myometrium: a patch clamp study. Prog Clin Biol Res 327:665–672

9. Fele-Zorz G et al (2008) A comparison of various linear and non-linear signal processing techniques to separate uterine EMG records of term and pre-term delivery groups. Med Biol Eng Comput 46:911–922

10. Garfield RE (1994) Role of cell-to-cell coupling in control of myometrial contractility and labor. In: Garfield RE, Tabb TN (eds) Control of uterine contractility. C.P.I. Llc., Florida

11. Hodgkin AL, Huxley AF (1952) A quantitative description of membrane current and its application to conduction and excitation in nerve. J Physiol 117(4):500–544

12. Inoue Y et al (1990) Some electrical properties of human pregnant myometrium. Am J Obstet Gynecol 162(4):1090–1098

13. Kao CY, McCullough JR (1975) Ionic currents in the uterine smooth muscle. J Physiol 246(1):1–36

14. Khan RN et al (2001) Potassium channels in the human myometrium. Exp Physiol 86(2):255–264. doi:10.1113/eph8602181

15. Knock G, Smirnov S, Aaronson P (1999) Voltage gated K⁺ currents in freshly isolated myocytes of the pregnant human myometrium. J Physiol 518:769–781. doi:10.1111/j.1469-7793.1999.0769p.x

16. Kuriyama H, Suzuki H (1976) Changes in electrical properties of rat myometrium during gestation and following hormonal treatments. J Physiol 260:315–333

17. Marshall J (1990) Relation between membrane potential and spontaneous contraction of the uterus, in uterine contractility: mechanisms of control. In: Garfield R, Norwell M (eds) Sereno symposia, pp 3–7

18. Marque C, Duchene J (1989) Human abdominal EHG processing for uterine contraction monitoring. Biotechnology 11:187–226

19. Marque C et al (1986) Uterine EHG processing for obstetrical monitoring. IEEE Trans Biomed Eng 33(12):1182–1187. doi: 10.1109/TBME.1986.325698

20. Miller SM, Garfield RE, Daniel EE (1989) Improved propagation in myometrium associated with gap junctions during parturition. Am J Physiol 256(1 Pt 1):C130–C141

21. Miyoshi H, Urabe T, Fujiwara A (1991) Electrophysiological properties of membrane currents in single myometrial cells isolated from pregnant rats. Pflugers Arch 419(3–4):386–393. doi:10.1007/BF00371121

22. Moore JW, Ramon F (1974) On numerical integration of the Hodgkin and Huxley equations for a membrane action potential. J Theor Biol 45(1):249–273. doi:10.1016/0022-5193(74)90054-X

23. Noble D (1962) A modification of the Hodgkin–Huxley equations applicable to Purkinje fibre action and pace-maker potentials. J Physiol 160:317–352

24. Ohya Y, Sperelakis N (1989) Fast Na⁺and slow Ca²⁺channels in single uterine muscle cells from pregnant rats. Am J Physiol 257(2 Pt 1):C408–C412

25. Parkington HC, Coleman HA (1988) Ionic mechanisms underlying action potentials in myometrium. Clin Exp Pharmacol Physiol 15(9):657–665. doi:10.1111/j.1440-1681.1988.tb01125.x

26. Ramon F et al (1976) A model of propagation of action potentials in smooth muscle. J Theor Biol 59:381–408. doi:10.1016/0022-5193(76)90178-8

27. Sanborn BM (1995) Ion channels and the control of myometrial electrical activity. Semin Perinatol 19(1):31–40. doi:10.1016/S0146-0005(95)80045-X

28. Sanborn BM (2000) Relationship of ion channel activity to control of myometrial calcium. J Soc Gynecol Investig 7(1):4–11. doi:10.1016/S1071-5576(99)00051-9

29. Shmigol A, Eisner D, Wray S (1998) Properties of voltage-activated [Ca²⁺]i transients in single smooth muscle cells isolated from pregnant rat uterus. J Physiol 511(3):803–811. doi:10.1111/j.1469-7793.1998.803bg.x

30. Sperelakis N, Inoue Y, Ohya Y (1992) Fast Na⁺channels and slow Ca²⁺ current in smooth muscle from pregnant rat uterus. Mol Cell Biochem 114(1–2):79–89. doi:10.1007/BF00240301

31. Wang R, Karpinski E, Pang PK (1989) Two types of calcium channels in isolated smooth muscle cells from rat tail artery. Am J Physiol 256(5 Pt 2):H1361–H1368

32. Wang SY et al (1998) Potassium currents in freshly dissociated uterine myocytes from nonpregnant and late-pregnant rats. J Gen Physiol 112(6):737–756. doi:10.1085/jgp.112.6.737

33. Yoshino M, Wang SY, Kao CY (1997) Sodium and calcium inward currents in freshly dissociated smooth myocytes of rat uterus. J Gen Physiol 110(5):565–577. doi:10.1085/jgp.110.5.565

34. Young RC (1997) A computer model of uterine contractions based on action potential propagation and intercellular calcium waves. Obstet Gynecol 89(4):604–608. doi:10.1016/S0029-7844(96)00502-9

35. Young RC, Herndon-Smith L (1991) Characterization of sodium channels in cultured human uterine smooth muscle cells. Am J Obstet Gynecol 164(1 Pt 1):175–181

36. Young RC, Smith LH, McLaren MD (1993) T-type and L-type calcium currents in freshly dispersed human uterine smooth muscle cells. Am J Obstet Gynecol 169(4):785–792